



Islamic Azad University  
Mashhad Branch

# The Effect of Estimation Methods on Multifractal Modeling for Mineralized Zone Delineation in the Dardevey Iron Ore Deposit, NE Iran

Peyman Afzal<sup>1\*</sup>, Shahab Shahbeik<sup>1</sup>, Parviz Moarefvand<sup>3</sup>, Amir Bijan Yasrebi<sup>2</sup>, Renguang Zuo<sup>4</sup>, Andrew Wetherelt<sup>2</sup>

1. Department of Mining Engineering, Faculty of Engineering, South Tehran Branch, Islamic Azad University, Tehran, Iran

2. Camborne School of Mines, University of Exeter, Penryn, UK

3. Amirkabir University of Technology, Mining and Metallurgy Faculty, Tehran, Iran

4. State Key Laboratory of Geological Processes and Mineral Resources, China University of Geosciences, Wuhan 430074, Beijing 100083, China

Received 16 July 2013; accepted 12 August 2013

## Abstract

The purpose of this study is to identify the effect of Ordinary Kriging (OK) and Inverse Distance Weighted (IDW) estimation methods for the delineation of mineralized zones based on subsurface data using concentration–volume (C–V) multifractal modeling in the Dardevey iron ore deposit, NE Iran. Variograms and anisotropic ellipsoids were generated for the Fe distribution using the above estimation methods. Continuity of ore and waste, the number of points involved, discretization factor for ore and waste boundaries and block model were generated for reserve estimation purposes. In addition, the C–V log–log plots based on the estimation methods that represent the various mineralized zones from existing thresholds and error estimations in both methods were compared. The comparison and interpretation of the mineralized zones based on the C–V fractal modeling show that the error is less in the OK method, although the volume of extreme, high and moderate zones resulting from the OK method is greater than the IDW method. The thresholds considering C–V fractal modeling for extremely, highly, moderately and weakly mineralized zones are 60.37%, 55.27% and 45.66% respectively for the OK method and 55.14%, 50.12% and 41.48% respectively for the IDW method. According to the threshold values, the error in the OK method is less than 20% while the error estimation resulting from the IDW method increases to 60%.

**Keywords:** Error estimation, JORC classification, Concentration–Volume (C–V) fractal modeling.

## 1. Introduction

Fractal/multifractal modeling has been widely applied in different geoscience branches especially in the spatial modeling of mineralized zones (e.g., [1-7]). The concentration-volume (C–V) fractal model by Afzal et al. (2011) can be utilized to distinguish between different mineralized zones with respect to the thresholds (breakpoints). As a result, the C–V fractal model is considered a proper method to describe spatial distributions of different attributes (ore elements in this scenario) within the various ore bodies [8 -10]. Geostatistical methods are commonly utilized for interpolation and estimation of different regional variables in 1D, 2D or 3D illustrations. Employment of an accurate estimation method with respect to geometry and geological properties of different deposits and drilling patterns is a problematic issue in reserve estimation [2, 11, 12]. Linear and non-linear kriging methods, Inverse Distance Weighted (IDW), interpolating polynomials, splines and power and Fourier series fitting have been created to overcome the

Above-mentioned problem [13 - 17]. In many cases, kriging has performed as the best estimator [18-24], while in others instances IDW or splines performed well [25- 29, 16]. There are many articles that compare Ordinary Kriging (OK) and IDW [12, 16]. Using real data rather than synthetic data has several advantages; it precludes one method from having an unfair advantage merely because the data used for the comparison are generated under the same model on which the method is based. On the other hand, only with synthetic data can the effect of certain data characteristics on interpolation accuracy be systematically evaluated [26, 22, 30, 16]. Evaluation of ore element distribution is an important parameter for mine planning and design [31]. Determination of estimation methods is essential for decreasing error estimation and increasing the accuracy of resource and reserve evaluation [32, 33]. Selection of an estimation method is essential for fractal/multifractal modeling, especially in the C–V model. On the other hand, accuracy of the estimation methods and their errors of interpolation affect the C–V fractal/multifractal modeling. The main aim of this paper is to separate out and compare the accuracy and error estimation of different mineralized zones which were derived using

\*Corresponding author.

E-mail address (es): P\_Afzal@azad.ac.ir

the C-V fractal model based on IDW and OK interpolation methods in the Dardevey iron ore deposit, in NE Iran. The C-V multifractal modeling and the interpolation methods including OK and IDW were used in this study.

## 2. Geological Setting of Dardevey Deposit

The Sangan iron ore complex is located approximately 300 Km SE of Mashhad, in NE Iran and is considered one of the greatest Iranian iron ore resources. The Sangan complex consists of several ore bodies such as Dardevey, Baghak, A, A', B, C, C North. The Dardevey deposit is situated approximately 18 km NE of Sangan, as shown in Fig.1. This area is located in the Lut structural zone, which is one of the subdivisions of the Iranian central structural zone at the north Darouneh fault, as depicted in Fig.1. Dardevey iron ore includes an Fe skarn system. The metallic minerals in the Dardevey deposit are magnetite, hematite, goethite, pyrite and martite [34].

The Dardevey deposit is located in the southern margin of the Upper Eocene Sar Nowsar granite (biotite-amphibole granite) and occurs in an east-west trending sequence of Upper Mesozoic sedimentary rock. The Magnetite skarn is formed in the black limestone and dolomite (Jurassic- Lower Cretaceous). They are considered massive and in some localities, they measure approximately 200m thick. Mineral paragenesis is magnetite ± hematite ± pyrite and some chalcopyrite ± garnet (andradite) ± actinolite ± chlorite ± phlogopite calcite ± dolomite. The Dardevey deposit is Mg-skarn with the Mg content of magnetite at around 1.22-1.26%. At least four stages of skarn formation and ore deposition have been documented in the area (stages I, II, III and IV a, b). Based on satellite images and field observation, the Dardevey deposit was displaced by a strike slip fault more than one kilometer from the Baghak deposit [35-37].

Exploration drill cores and surface magnetic surveys in the study area confirmed that the motion and dips of the mineralized zone are inclined towards the South (80°-85°). The recognition of a fault system and structural features is important because these may materially affect the assessment and exploration of other segments of the hidden ore body. In addition, the main structural features include two fault systems trending NW-SE and E-W, as depicted in (Fig. 2: [35]).

## 3. Methodology

The concentration-volume (C-V) fractal model proposed by [1] is utilized to delineate the various mineralized zones in order to characterize the distribution of major, minor and trace element concentrations in relation to the Iranian Cu porphyry deposits (Sungun and Chah-Firuzeh). This model is expressed in the following form:

$$V(\rho \leq v) \propto \rho^{-a_1}; V(\rho \geq v) \propto \rho^{-a_2} (1)$$

Where,  $V(\rho \leq v)$  and  $V(\rho \geq v)$  indicate volumes (V) with concentration values ( $\rho$ ) that are, respectively, smaller and greater than contour values ( $v$ ), which define those volumes, and  $a_1$  and  $a_2$  are exponents. In the log-log plots of concentration values versus volumes, certain concentration contours representing breakpoints in the plots are considered threshold values which distinguish the mineralized zones located in the different types of the ore deposit. In the C-V model, breakpoints between straight-line segments in the log-log plots represent threshold values separating populations of geochemical concentration values that represent mineralized zones according to distinct geochemical processes [1-2]. Threshold values are recognized by applying the fractal C-V model likely to represent the boundaries between different ore zones [4, 1, 9, 10].

To calculate  $V(\rho \leq v)$  and  $V(\rho \geq v)$  enclosed by a concentration contour in a 3D model, e.g., the original drill core data of the ore element, concentrations were interpolated using the IDW and OK estimation methods. Geostatistical techniques such as OK and IDW are widely used for ore grade estimation [39].

Kriging is among a group of geostatistical methods used for the interpolation of different regional variable values (e.g., ore element in this case) which consist of OK, universal kriging, indicator kriging, co-kriging and others [40-43]. OK and non-linear geostatistical estimators are proper methods in ore control and reserve/resource estimation where kriging is commonly described as a "minimum variance estimator" [44]. The choice of which kriging method should be used depends on the characteristics of the data and the type of spatial model. The most common geostatistical method is OK which was selected for this study. OK plays a special role because of its compatibility with a stationary model which involves a variogram [45, 1, 46]. OK estimates based on a moving average of the variable of interest satisfy various dispersion forms of data e.g. sparse sampling points. Moreover, it is a linear model based on local neighborhood structure [47, 39].

## 4. Variography and Anisotropic Ellipsoid

Variograms and anisotropic ellipsoids are a set of widely used statistical tools for spatial estimation and interpolation, which are the fundamental components for geostatistical modeling [48, 49]. Based on 156 drill cores (Fig. 3) and 5,922 collected samples 2 m in length, the non-directional and directional variograms were generated using Datamine Studio Software v. 3.19, as shown in Table 1 and Fig. 4. Moreover, the histogram of Fe was generated by SPSS which shows a multimodal distribution for Fe in the area, as depicted in Fig. 3. Finally, anisotropic ellipsoids and the axis characteristics were also provided (Table 2 and Fig.5).

The main axis of the anisotropic ellipsoid shows trends in the N119 and N323 with 244 and 45 m ranges. The search ratios of the estimation are 0.75 of these ranges.

## 5. Determination of Evaluation Parameters

Three evaluation parameters were calculated as follow:

A) Continuity of ore and waste.

B) Optimization of the number of points involved in the estimation of ore and waste boundaries.

C) Optimization of the discretization factor in the estimation of ore and waste boundaries.

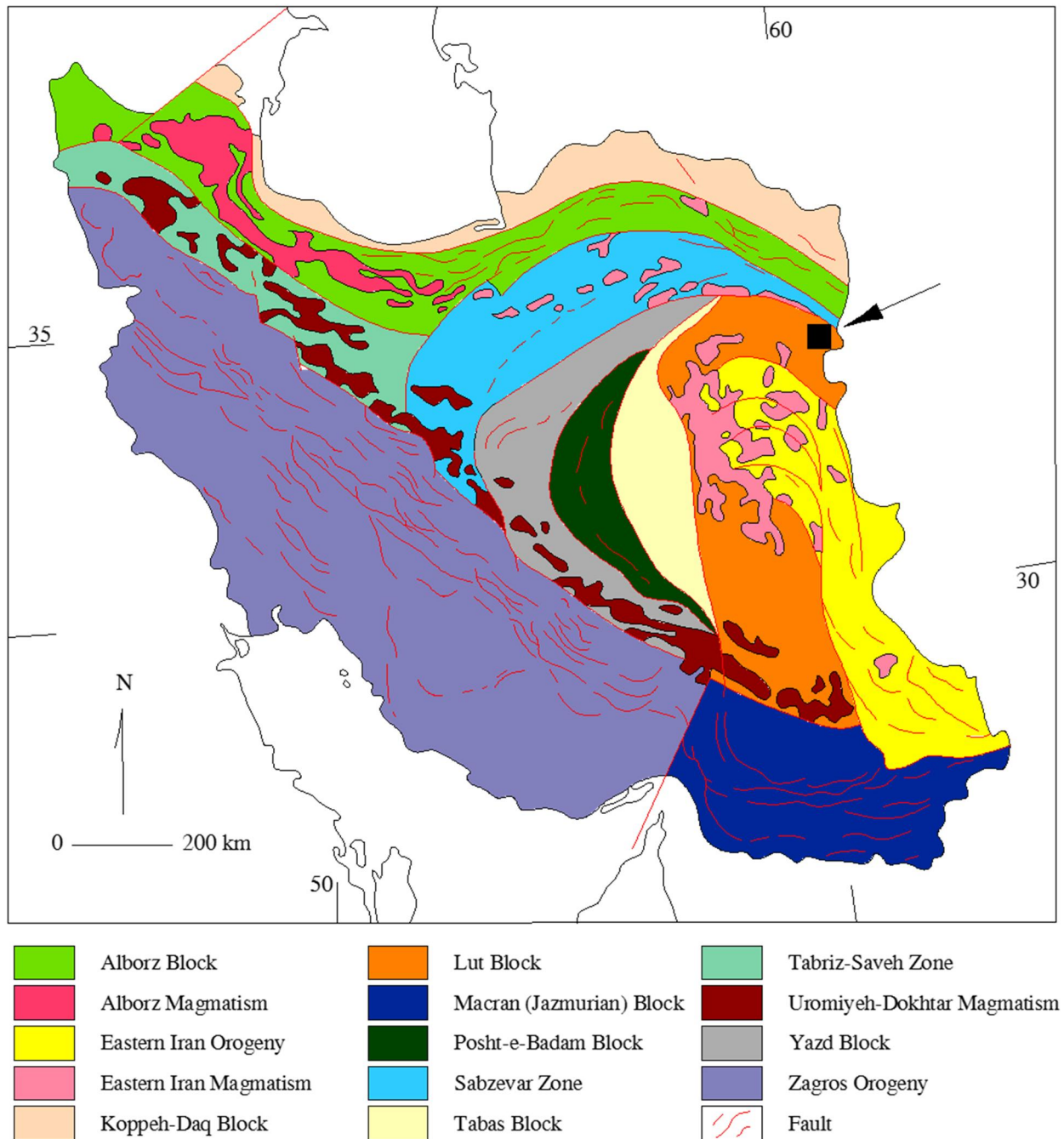


Fig. 1. Location of studied area in structural map of Iran (Black Square; [38])

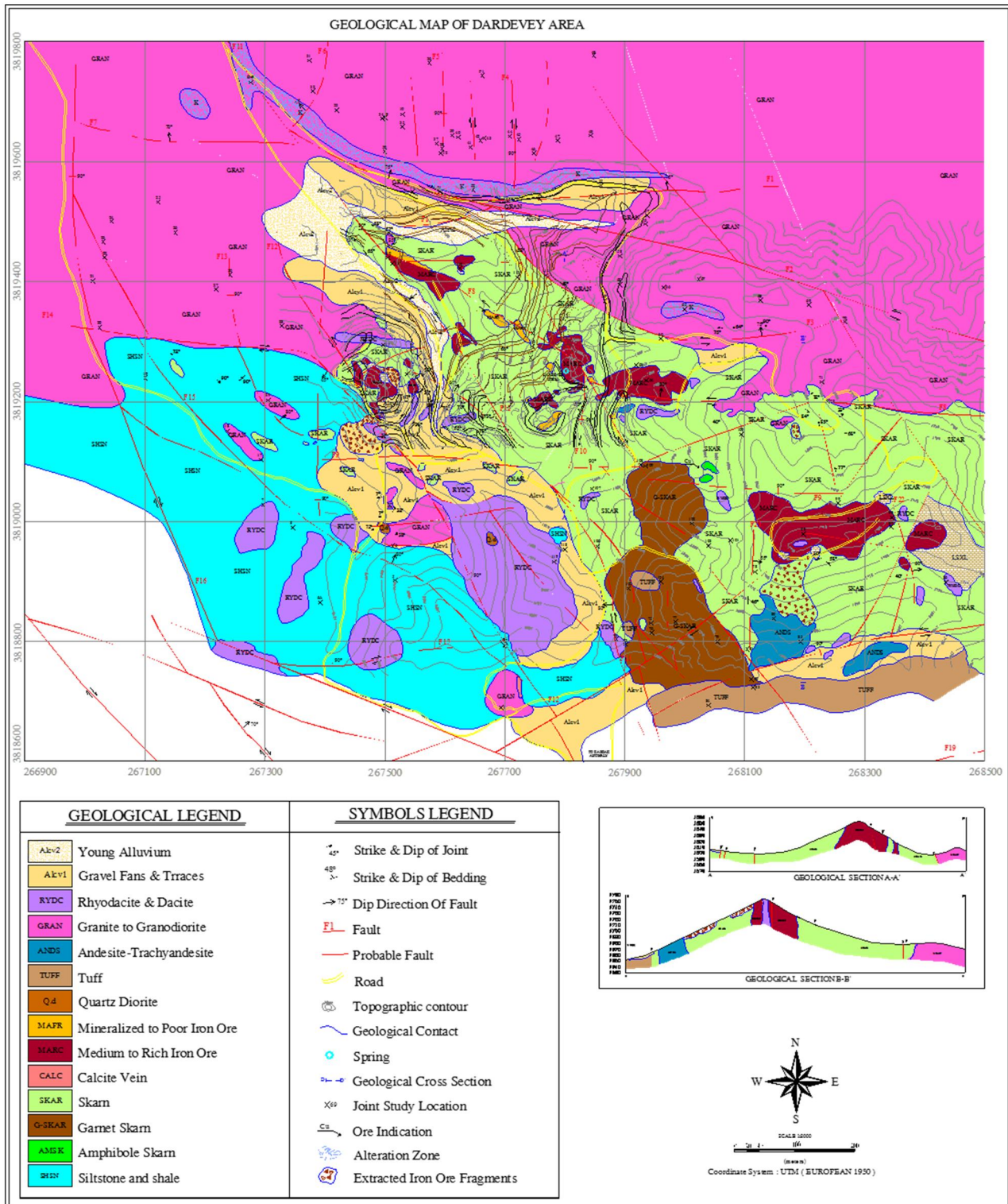


Fig. 2. Geological and structural map of studied area [34]

Table 1. Result of non-directional and directional variograms

Variables	Range	C-Value	Sill	Nugget Effect
Non-Direction	412.8	45.3	147.2	101.9
Axis 1	244.8	64.1	148	83.9
Axis 2	113.4	40.2	131.1	90.9
Axis 3	45.7	56.7	111.2	54.5

Table 2. Anisotropic ellipsoid particulars in the deposit

Variables	Azimuth	Dip
Axis 1	119.49	-4.00
Axis 2	209.62	-1.78
Axis 3	323.56	-85.62

### 3-1. Continuity of ore and waste

Thickness continuity of ore and waste in reserve estimation plays an essential role which is a function of grade continuity. The degree of continuity of grade in the mineralization is a function of the mineralization type. For example, in sedimentary mineralization with layered geometry, continuity in directions X and Y (length and width of the deposit) to Z (the thickness of the deposit) has a higher degree [50].

Fe grades of 20% were considered for the determination of the extent of waste and ore. According to this criterion, the Fe values measured in each drill core were allocated to either waste or ore (0 and 1 respectively). In addition, the continuous thickness of the ore and waste was measured. The value of continuity was calculated in the composites at 1, 2.5, 5, 10, 15 and 20 meters (Fig. 6). Based on these estimates and assessments, voxels should not be more than 5 meters in height due to the increased stripping ratio.

### 3-2. Optimizing the number of points involved in the estimation of ore and waste boundaries

The minimum and maximum numbers of points involved in the estimation of each voxel are the important parameters [51, 52, 53]. To select the optimum number of points, a minimum number of points (2, 4, 6 and 8) and a maximum number (10, 12, 14, 16, 18 and 20) were tested in each case. Based on these estimations, the minimum number of 2 points and the maximum number of 10 points with accuracies of 81.53% as the number of optimal points for estimation of ore and waste boundaries were selected (Table 3). The results of the validation are shown in Fig. 7.

### 3-3. Optimizing the discretization factor in the estimation of ore and waste boundaries

It is essential to select the optimal discretization factor in the estimation of a 3D block model. Most of the geostatistical software packages, e.g. Datamine, are estimated with respect to points. By applying this parameter, the results are generally closer to the values of the estimated block [54, 55]. Next, the Fe values are estimated with different discretization factors based on the previously mentioned parameters (Table 4). The average of the estimated variance in the discretization factor of  $5 \times 5 \times 5\text{m}^3$  is less than the other scenarios which were examined and therefore, this factor was chosen as the optimal factor (Table 4).

Table 3. Different models to select the number of points involved in the estimation of ore and waste boundaries

Row	Minimum Point No.	Maximum Point No.	Accuracy
1	2	10	81.53%
2	2	12	81.47%
3	2	14	81.41%
4	2	16	81.34%
5	2	18	81.29%
6	2	20	81.30%
7	4	10	81.50%
8	4	12	81.46%
9	4	14	81.40%
10	4	16	81.32%
11	4	18	81.28%
12	4	20	81.29%
13	6	10	81.50%
14	6	12	81.46%
15	6	14	81.40%
16	6	16	81.33%
17	6	18	81.28%
18	6	20	81.29%
19	8	10	81.50%
20	8	12	81.46%
21	8	14	81.40%
22	8	16	81.33%
23	8	18	81.28%
24	8	20	81.29%

Table 4. Result of optimization of discretization factor with the average variance of the estimations

Discretization Factor	Average of Variance
3×3×3	57.59
4×4×4	57.36
5×5×5	57.21

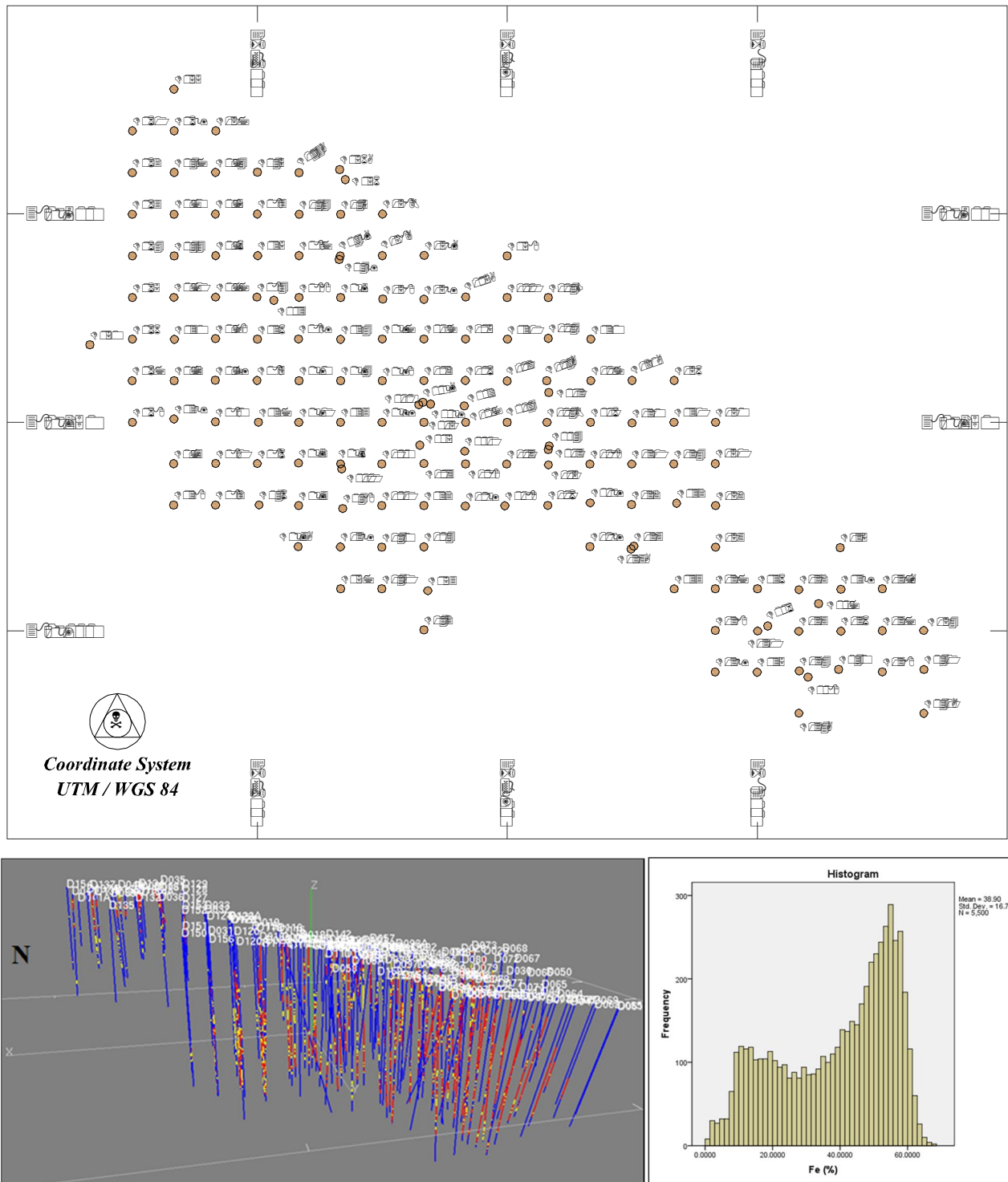


Fig. 3. 2D and 3D grid drilling in the Dardevey deposit and histogram of Fe data

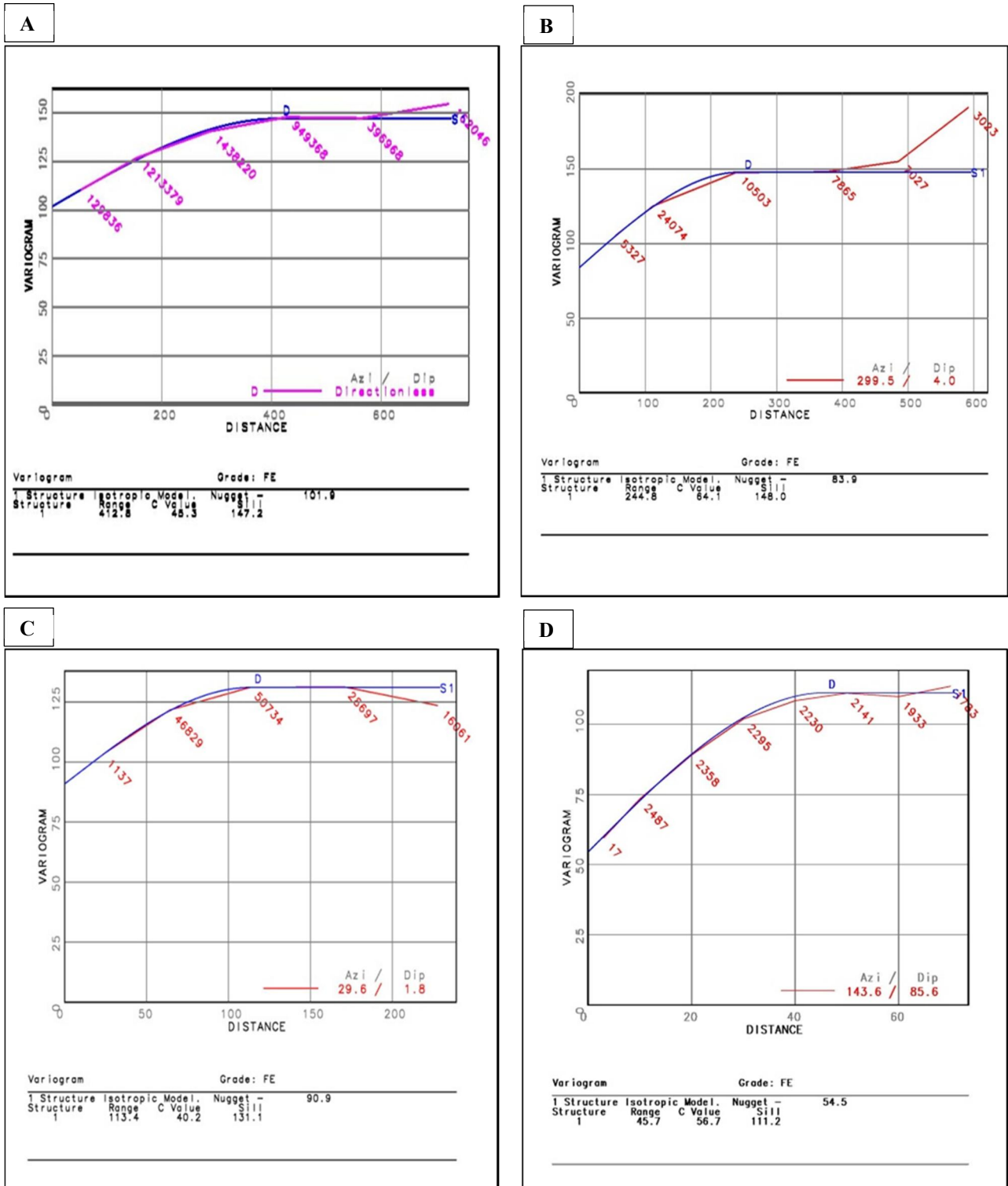


Fig. 4. Non-directional and directional variograms; A) Non-directional, B) Axis 1, C) Axis 2 and D) Axis 3

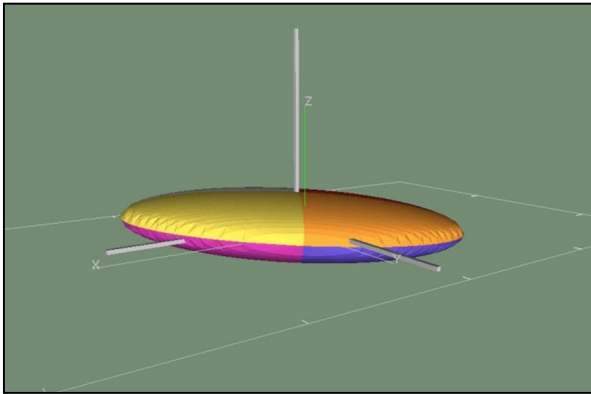


Fig. 5. Anisotropic ellipsoid in the Dardevey deposit

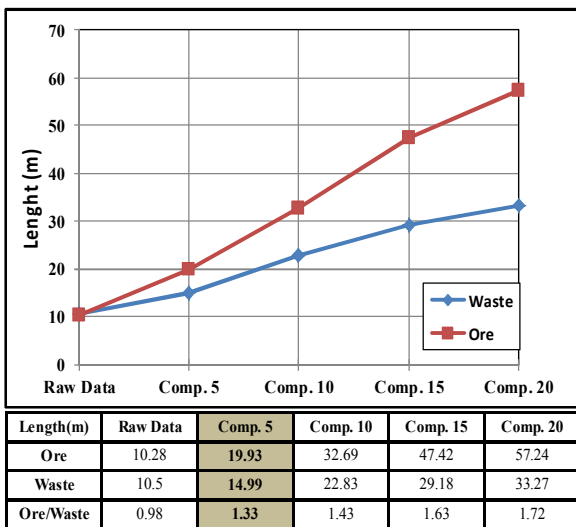


Fig. 6. Continuity of ore and waste in different composites

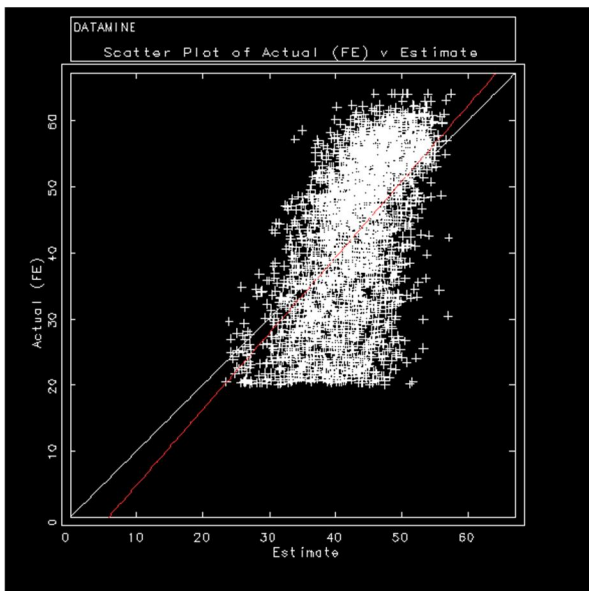


Fig. 7. Validation of the number of point's optimum for the estimation of ore and waste boundaries

#### 4. Block Modeling

Determination of the various voxel dimensions within the 3D block model is important for reserve evaluation and mine planning. [56] proposed using a general method for the operation due to the geometrical particulars of a deposit and grid drilling. As a result, the voxels' dimensions were calculated as follows:

- A) Length of each voxel is 25 m, which is equal to half of the distance between the drill cores in regard to the least variability (longitudinal direction) of the deposit.
- B) Width of each voxel is 12.5 meters, which is a quarter of the distance between the drill cores.
- C) Height of each voxel is 5 meters due to the continuity of ore and waste thickness.

After determining the optimal size for each voxel, a 3D block model of the deposit was generated as illustrated in Fig. 8.

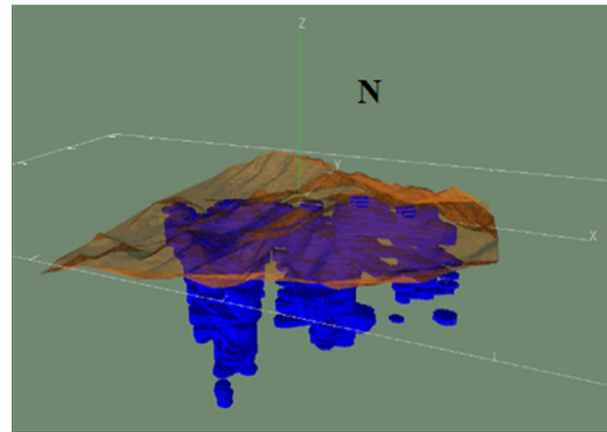


Fig. 8. 3D block model of the Dardevey deposit

#### Evaluation by OK and IDW

According to variography, the block model for Fe values in the deposit was built up using both the OK and IDW methods. However, estimation methods have the weakness of both overestimation and underestimation in areas where there is not an adequate amount of data due to the lack of drill core information. The density of sampling points along the boreholes is very high, however, the sampling information between holes is very limited. Therefore, there is often an undesired overestimation or underestimation when estimating points along the drill cores [57]. This problem is obvious in the cumulative distribution function of the estimated element (Fe). To solve this problem, the cumulative distribution function of the estimated values and the original values of each variable (composite) were proposed and used. The results are shown in Fig. 9. The function corrects the points of overestimation and underestimation based on the initial amount found using the OK method. This equation in which  $Fe_c$  and  $Fe_e$  are the corrected and



estimated values respectively is as follows:

$$Fe_c = -1937014.3 + 2535647.8 Fe_e^{0.5} - 1418173.4 Fe_e + 435411.46 Fe_e^{1.5} - 77044.283 Fe_e^2 + 6973.4109 Fe_e^{2.5} - 31.637299 Fe_e^3 - 62.705574 Fe_e^{3.5} + 6.5279055 Fe_e^4 - 0.2834302 Fe_e^{4.5} + 0.0045392155 Fe_e^5(2)$$

After correction of the assay values for both methods, a grade-tonnage curve was generated for the different assays as illustrated in Fig. 10.

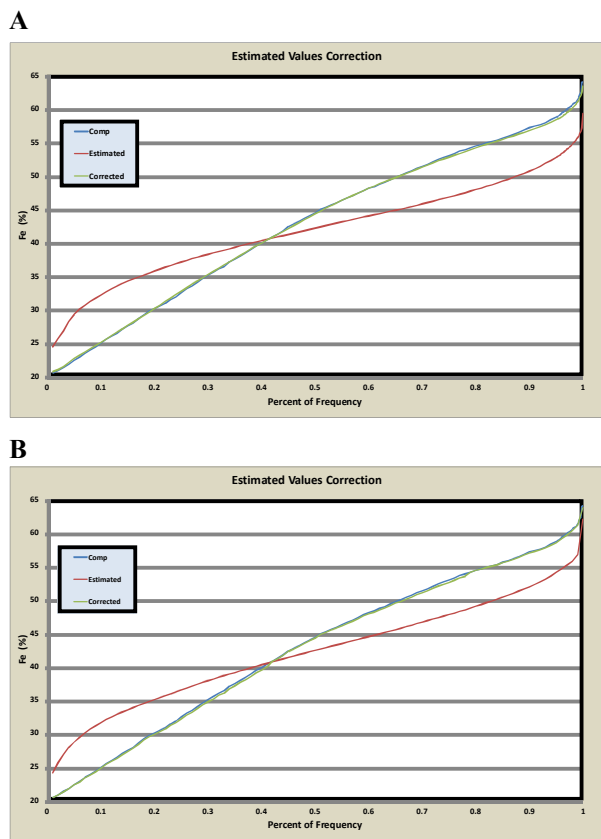


Fig. 9. Correction of estimated values of Fe variable; A) OK method, B) IDW method

**C–V Fractal Modeling**

Based on the 3D models of the deposit using both the IDW and OK methods, volumes corresponding to the different Fe grades were calculated to derive a C–V fractal model. Threshold values of Fe were recognized in the C–V log–log plots for both methods (Fig. 11), which revealed a power-law relationship between Fe concentrations and volumes occupied. The depicted arrows in the log–log plots show three distinct threshold values (breakpoints) corresponding to 45.66%, 55.27% and 60.37% respectively of Fe using the OK method and 41.48%, 50.12% and 55.14% of Fe using the IDW method. For each method based on the log–log plots, mineralized zones were separated into four distinct categories: extremely, highly, moderately and weakly mineralized zones, as shown in Table 5.

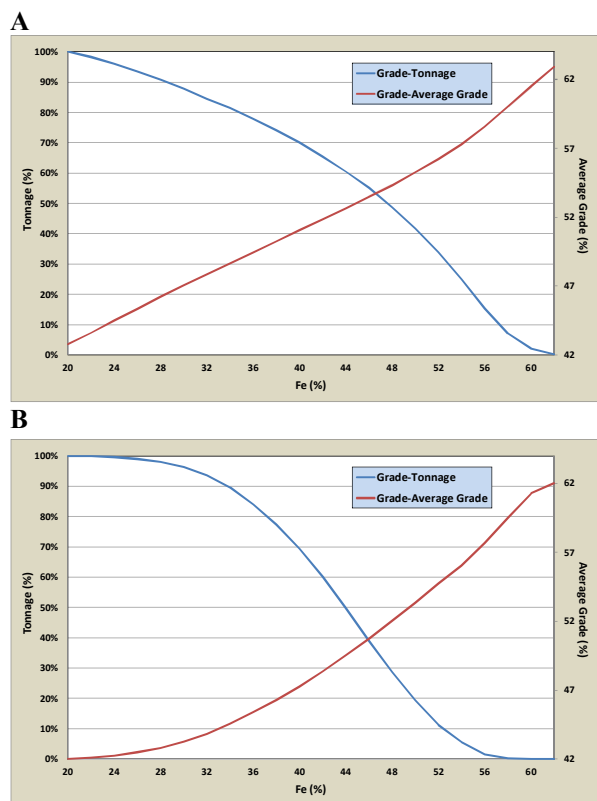


Fig. 10. Curve of grade-tonnage; A) OK method and B) IDW method

According to the C–V fractal model, most of the extremely and highly mineralized zones were situated in the SE part of the deposit (Fig. 12). However, small highly mineralized zones were found in the NW part of the deposit. It would seem that the major mineralization has a trend of NW – SE.

Table 5. Separation of mineralized zones in the Dardevey deposit based on three thresholds of Fe contents defined from the C–V fractal model

<i>OK Method</i>	
Mineralized zones	Range Fe (%)
Extremely Mineralized Zone	Fe ≥ 60.37
Highly Mineralized Zone	55.27 ≤ Fe ≤ 60.37
Moderate Mineralized Zone	45.66 ≤ Fe ≤ 55.27
Weakly Mineralized Zone	Fe ≤ 45.66
<i>IDW Method</i>	
Mineralized zones	Range Fe (%)
Extremely Mineralized Zone	Fe ≥ 55.14
Highly Mineralized Zone	50.12 ≤ Fe ≤ 55.14
Moderate Mineralized Zone	41.48 ≤ Fe ≤ 50.12
Weakly Mineralized Zone	Fe ≤ 41.48

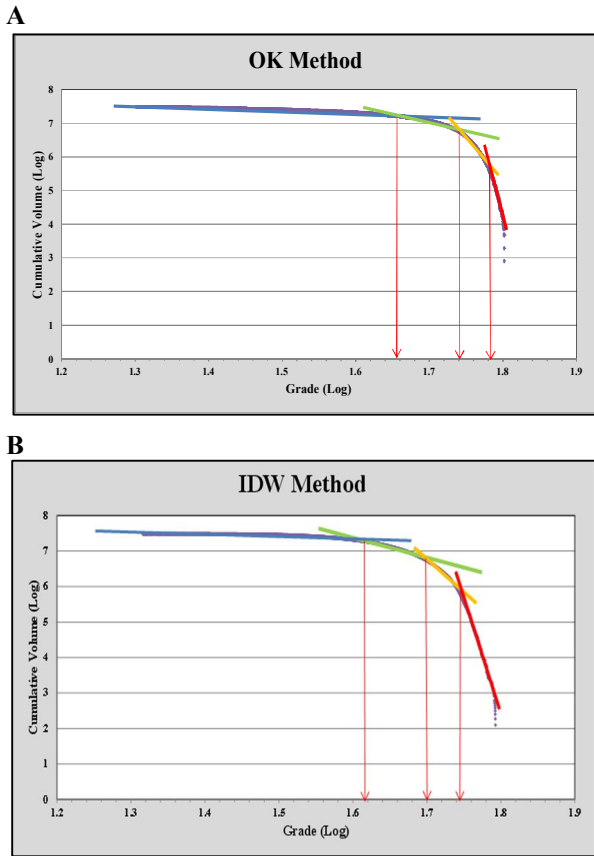


Fig. 11. C-V log-log plot for Fe concentrations based on OK and IDW methods.

**Error Estimation and Classification of C-V Mineralized Zones**

In ore estimation it is necessary to calculate the error of each voxel and the classification of reserves. The following formula for calculation of the estimation error is used [58 - 61]:

$$\% \text{ Error} = \left( \frac{Z \cdot S}{x \cdot \sqrt{N}} \right) \times 100 \quad (3)$$

S, X and V are the standard deviations of each voxel, assay of each voxel and the number of samples that are participating in the grade estimation, respectively. Z is the integer constant, which is 1.96 if the confidence level is 95% or 1.64 if the confidence level is 90%. In this study, the confidence level assigned to Z was 90% hence a Z of 1.64 was used.

The reserves estimated by both the IDW and OK methods are classified based on error estimation. The JORC [62] method was selected to classify the reserves, as shown in Tables 6 and 7. The classification framework, based on the prepared code by the Joint Ore Reserves Committee of the Australasian Institute of Mining and Metallurgy, Australian Institute of Geoscientists and Minerals Council of Australia (JORC code), which is one of the international standards for mineral resource and ore reserve reporting, provides a template system that conforms to international society

requirements [63, 64].

Most estimated voxels using the OK method had low values of error, which were generally lower than 20% (Table 6) while several evaluated voxels by the IDW method (about 19%) had error estimations between 20 and 40% (Table 7). Most parts of the estimated block model derived via the OK method (higher than 99.7%) were classified in the A category based on JORC standard (Table 6). However, about 19% of the estimated tonnages using the IDW method were categorized in the B class (Table 7). Extremely, highly and moderately mineralized zones obtained by the C-V model based on the OK estimation method had lower values of error, (lower than 20%). There are very low values of weakly mineralized zones (0.22%) with errors more than 20%, as depicted in Table 6. Unlike the OK method, more than 15% of the mineralized zones derived via the C-V modeling from the IDW block model have error estimations greater than 20%, especially between 20-40% (Table 7). Based on these results, the C-V fractal modeling based on the estimated data from the OK method generally has higher accuracy compared to the IDW estimated block model.

Table 6. Reserves classification based on JORC standard in OK method

<i>Greater than 60.37% (Extremely zone)</i>			
Error	Average Grade (%)	Tonnage (%)	Classification
0% - 20%	61.42	1.63	A
20% - 40%	-	-	B
40% - 60%	-	-	C
> 60%	-	-	Possible
<b>Grand Total</b>	<b>61.42</b>	<b>1.63</b>	
<i>Between 55.27% and 60.37% (Highly zone)</i>			
Error	Average Grade (%)	Tonnage (%)	Classification
0% - 20%	57.30	17.23	A
20% - 40%	-	-	B
40% - 60%	-	-	C
> 60%	-	-	Possible
<b>Grand Total</b>	<b>57.30</b>	<b>17.23</b>	
<i>Between 45.66% and 55.27% (Moderate zone)</i>			
Error	Average Grade (%)	Tonnage (%)	Classification
0% - 20%	50.79	37.15	A
20% - 40%	-	-	B
40% - 60%	-	-	C
> 60%	-	-	Possible
<b>Grand Total</b>	<b>50.79</b>	<b>37.15</b>	
<i>Less than 45.66% (Weakly zone)</i>			
Error	Average Grade (%)	Tonnage (%)	Classification
0% - 20%	33.46	43.78	A
20% - 40%	21.51	0.12	B
40% - 60%	20.27	0.10	C
> 60%	-	-	Possible
<b>Grand Total</b>	<b>33.30</b>	<b>54675513.36</b>	

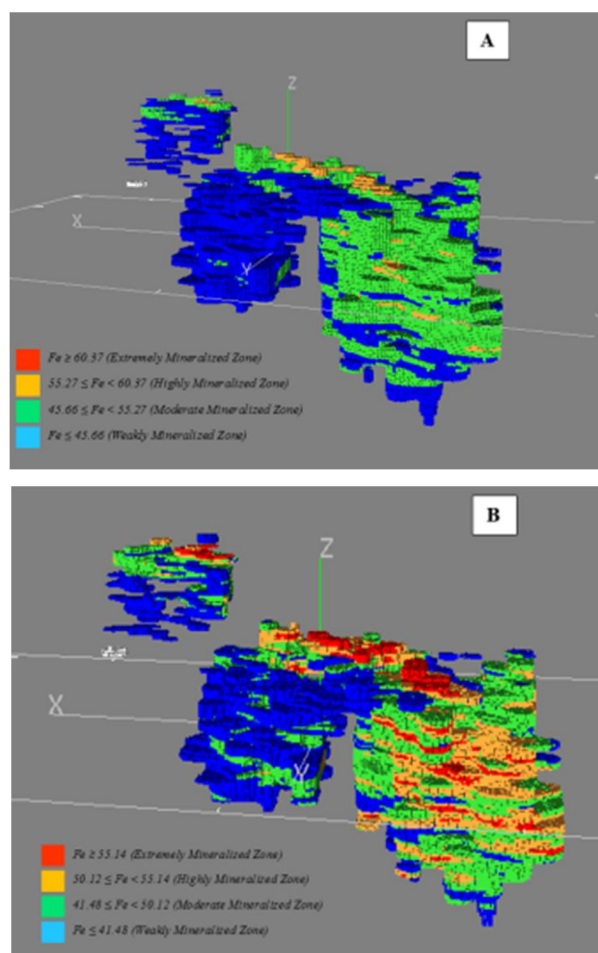


Fig. 12. Separation of mineralized zones based on thresholds defined from the C-V fractal model; A) OK method, B) IDW method.

## Conclusions

Choosing the proper method for reserve estimation with the minimum error is important in any geostatistical and fractal/multifractal modeling. Most of the fractal/multifractal models were defined based on estimated data and the determination of a robust method to estimate various types of data distributions such as geochemical data. In this study, the block models obtained from OK and IDW estimation methods were generated and the error distribution in both methods was examined within the deposit by considering the C-V fractal model. Based on the JORC standard, the error of the OK method was less than the IDW technique in the C-V mineralized zones outlining that 99.78% of the reserve had errors less than 20%. Extremely, highly and moderately mineralized zones have error estimations lower than 20% in the block model constructed by OK. Based on the results obtained using the IDW method, 19% of the C-V mineralized zones have errors between 20 to 40%. As a result, error estimation in the C-V mineralized zones

based on the OK block model is lower than the C-V mineralized zones obtained using the IDW estimation method. Therefore, the C-V modeling based on the OK estimated block model has accuracies higher than those resulting from the IDW technique due to the estimation errors calculated in the Dardevey iron ore deposit.

Table 7. Reserves classification based on JORC standard in IDW method

<i>Greater than 55.14% (Extremely zone)</i>			
Error	Average Grade (%)	Tonnage (%)	Classification
0% - 20%	56.52	1.26	A
20% - 40%	56.03	0.13	B
40% - 60%	-	-	C
> 60%	-	-	Possible
<b>Grand Total</b>	<b>56.47</b>	<b>1.38</b>	
<i>Between 55.14% and 50.12% (Highly zone)</i>			
Error	Average Grade (%)	Tonnage (%)	Classification
0% - 20%	52.32	6.52	A
20% - 40%	52.20	2.16	B
40% - 60%	52.57	0.01	C
> 60%	-	-	Possible
<b>Grand Total</b>	<b>52.28</b>	<b>8.69</b>	
<i>Between 41.48% and 50.12% (Moderate zone)</i>			
Error	Average Grade (%)	Tonnage (%)	Classification
0% - 20%	45.52	28.29	A
20% - 40%	45.75	8.45	B
40% - 60%	49.49	0.003	C
> 60%	-	-	Possible
<b>Grand Total</b>	<b>45.59</b>	<b>36.74</b>	
<i>Less than 41.48% (Weakly zone)</i>			
Error	Average Grade (%)	Tonnage (%)	Classification
0% - 20%	34.83	45.14	A
20% - 40%	36.12	8.04	B
40% - 60%	-	-	C
> 60%	-	-	Possible
<b>Grand Total</b>	<b>35.08</b>	<b>53.18</b>	

## Acknowledgments

The authors would like to thank Mr. Ravanbakhsh Amiri, Executive Manager of the Iran East Iron Ore Company (IEIOC) for authorizing the use of the Dardevey exploration dataset and Mrs. Mania Qumarsy for her contribution to the reserve estimation. The authors also would like to acknowledge Mr. Farzan Rafia, Mr. Alireza Shivaei, Mr. Ali Hooman Arabshahi, Mr. Mohammad Seydi and Mrs. Mona Zandi, as well as the managers and personnel of

Kavoshgaran Consulting Engineers Company for their professional advice.

## References

- [1] Afzal, P., FadakarAlghalandis, Y., Khakzad, A., Moarefvand, P., RashidnejadOmran, N. (2011) Delineation of mineralization zones in porphyry Cu deposits by fractal concentration–volume modeling. *J GeochemExplor*, v. 108, pp. 220–232.
- [2] Afzal, P., FadakarAlghalandis, Y., Moarefvand, P., Rashidnejad Omran, N., AsadiHaroni, H. (2012) Application of power-spectrum–volume fractal method for detecting hypogene, supergene enrichment, leached and barren zones in Kahang Cu porphyry deposit, Central Iran. *J Geochem Explor*, v. 112, pp. 131-138.
- [3] Agterberg, F.P. (1995) Multifractal modeling of the sizes and grades of giant and supergiant deposits. *IntGeol Rev*, v. 37, pp. 1–8.
- [4] Delavar, S. T., Afzal, P., Borg, G., Rasa, I., Lotfi, M., Rashid nejad Omran, N. (2012) Delineation of mineralization zones using concentration–volume fractal method in Pb–Zn carbonate hosted deposits. *J GeochemExplor*, v. 118, pp. 98-110.
- [5] Heidari, M., Ghaderi, M., Afzal, P. (2013) Delineating mineralized phases based on lithogeochemical data using multifractal model in Touzlar epithermal Au-Ag (Cu) deposit, NW Iran. *Appl Geo chem*, v.31, pp. 119-132.
- [6] Wang, Q.F., Deng, J., Liu, H., Wang, Y., Sun, X., Wan, L. (2011) Fractal models for estimating local reserves with different mineralization qualities and spatial variations. *J GeochemExplor*, v. 108, pp. 196–208.
- [7] Wang, G., Carranza, E. J. M., Zuo, R., Hao, Y., Du, Y., Pang, Zh., Sun, Y., Qu, J. (2012) Mapping of district-scale potential targets using fractal models. *J Geochem Explor*, v. 122, pp. 34-46.
- [8] DaneshvarSaein, L., Rasa, I., Rashidnejad Omran, N., Moarefvand, P., Afzal, P. (2012) Application of concentration-volume fractal method in induced polarization and resistivity data interpretation for Cu-Mo porphyry deposits exploration, case study: Nowchun Cu-Mo deposit, SE Iran. *Nonlin Processes in Geophys.* v. 19, pp. 431–438.
- [9] Sadeghi, B., Moarefvand, P., Afzal, P., Yasrebi, A. B., DaneshvarSaein, L. (2012) Application of fractal models to outline mineralized zones in the Zaghia iron ore deposit, Central Iran. *J Geochem Explor*, v. 122, pp. 9-19.
- [10] Yasrebi, A.B., Afzal, P., Wetherelt, A., Foster, P., Esfahanipour, R. (2013) Correlation between geology and concentration-volume fractal models: significance for Cu and Mo mineralized zones separation in the Kahang porphyry deposit (Central Iran) *Geologica Carpathica*. v.64, 153-163.
- [11] David, M. (1970a) Geostatistical estimation of porphyry-type deposits and scale factor problem. *Proceedings, Pribram Mining Symposium*. Pribram, Czechoslovakia.
- [12] Yasrebi, J., Saffari, M., Fathi, H., Karimian, N., Moazallahi, M., Gazni, R. (2009) Evaluation and Comparison of Ordinary Kriging and Inverse Distance Weighting Methods for Prediction of Spatial Variability of Some Chemical Parameters. *Research J of BiolSci*, v. 4, pp. 93–102.
- [13] Franke, R.(1982) Scattered data interpolation: tests of some methods. *Math Comp*, vol.38, pp. 181–200.
- [14] Lam, N. S. (1983) Spatial interpolation methods: A review. *AmerCartog*, v.10, pp. 129–149.
- [15] Cressie, N.(1993) *Statistics for spatial data*. John Wiley & Sons, New York, 900 p.
- [16] Zimmerman, D., Pavlik, C., Ruggles, A., Armstrong, M.P. (1999) An Experimental comparison of ordinary and universal kriging and inverse distance weighting. *Math Geol*, v.31, pp. 375–390.
- [17] Juan, P., Mateu, J., Jordan, M.M., Mataix-Solera, J., Meléndez-Pastor, I., Navarro-Pedreño, J.(2011) Geostatistical methods to identify and map spatial variations of soil salinity. *J GeochemExplor*, v. 108, pp. 62-72.
- [18] Matheron, G. (1967) Kriging or polynomial interpolation procedures. *C.I.M. Bulletin*, v. 60, no. 655, pp. 1041-1045.
- [19] Marechal, A., Serra, J. (1971) *Random Kriging*. Geostatistics, D.F. Merriam Editor, Plenum Press, New York.
- [20] Rouhani, S. (1986) Comparative study of ground-water mapping techniques. *Ground Water*, v. 24, pp. 207–216.
- [21] Laslett, G.M., and McBratney, A.B. (1990) Further comparison of spatial methods for predicting soil pH. *Soil SciSoc America J*, v. 54, pp. 1553–1558.
- [22] Weber, D.D., Englund, E.J. (1994) Evaluation and comparison of spatial interpolators, II. *Math. Geol.* v. 26, pp. 589–603.
- [23] Laslett, G.M. (1994) Kriging and splines: An empirical comparison of their predictive performance in some applications. *Jour. Am. Stat. Assoc*, v. 89, pp. 391–409.
- [24] Phillips, D.L., Lee, E.H., Herstrom, A.A., Hogsett, W.E., and Tingey, D.T. (1997) Use of auxiliary data for spatial interpolation of ozone exposure in southeastern forests. *Environmetrics*, v.8, pp. 43–61.
- [25] Laslett, G. M., McBratney, A. B., Pahl, P. J., Hutchinson, M. F. (1987) Comparison of several spatial prediction methods for soil pH: *Jour. of Soil Sci*, v. 38, no. 2, pp. 325–341.
- [26] Weber, D.D., Englund, E.J. (1992) Evaluation and comparison of spatial interpolators. *Math. Geol.* v.24, pp. 381–391.
- [27] Gallichand, J., and Marcotte, D. (1993) Mapping clay content for subsurface drainage in the Nile delta. *Geoderma*, v. 58, nos. 3/4, pp. 165–179.
- [28] Brus, D. J., de Gruijter, J. J., Marsman, B. A., Visschers, R., Bregt, A. K., and Breeuwsma, A. (1996) The performance of spatial interpolation methods and choropleth maps to estimate properties at points: A soil survey case study. *Environmetrics*. v.7, pp. 1–16.
- [29] Declercq, F. A. N. (1996) Interpolation methods for scattered sample data: Accuracy, spatial patterns, processing time. *Cartography and GeogInf Sys*, vol. 23, no. 3, p. 128–144.
- [30] Englund, E.J., Weber, D.D., Leviant, N. (1992) The effects of sampling design parameters on block selection. *Math. Geol.* v. 24, pp. 29–343.
- [31] Hustrulid, W.A., Kochta, M. (2006) *Open pit mine planning and Design* (Second Ed.). Taylor & Francis; 991 p.
- [32] Dimitrakopoulos, R., Martinez, L., Ramazan, S. (2007) A maximum upside/minimum downside approach to the

- traditional optimization of open pit mine design. *J Min Sciv.* 43, no. 1, pp. 73-82.
- [33] Parhizkar, A., Ataei, M., Moarefvand, P., and Rasouli, V. (2011) Grade Uncertainty and Its Impact on Ore Grade Reconciliation Between the Resource Model and the Mine. *Arch. Min. Sci.* v. 56, pp. 119-134.
- [34] Hasanipack, A.A., Halaji, A., Rajaeian, F. (2009) Modeling and reserve evaluation of Dardevey deposit, Madankav Co. (Persian Unpublished report).
- [35] Ghavi, J., Karimpour, M.H. (2010) Geological Investigation and Mineralization of the Dardvey Iron deposit, Sangan Ore Field, Northeast Iran. The First International Applied Geological Congress Proceeding, Department of Geology, Islamic Azad University - Mashad Branch, Iran, pp. 26-28.
- [36] Malekzadeh Shafaroudi, A., Karimpour, M.H., Golmohammadi, A., 2013. Zircon U-Pb geochronology and petrology of intrusive rocks in the C-North and Baghak districts, Sangan iron mine, NE Iran. *Journal of Asian Earth Sciences* 64: 256-271
- [37] Golmohammadi, A., Karimpour, M.H., Malekzadeh Shafaroudi, A., Mazaheri, S.A., 2014. Alteration-mineralization, and radiometric ages of the source pluton at the Sangan iron skarn deposit, northeastern Iran. *Ore Geology Reviews* (In press).
- [38] Stocklin, J.O. (1977) Structural correlation of the Alpine ranges between Iran and Central Asia. *Memoir Hors Service Societe Geologique France*, v. 8, pp. 333-353.
- [39] Tahmasebi, P., Hezarkhani, A. (2010) Application of Adaptive Neuro-Fuzzy Inference System for Grade Estimation; Case Study, Sarcheshmeh Porphyry Copper Deposit, Kerman, Iran. *Aust J of Basic and Appl Sci*, v.4, pp. 408-420.
- [40] Bayraktar, H., Turalioglu, F.S. (2005) Kriging-based approaches for locating a sampling site-in the assessment of air quality. *SERRA*, v.19, no.4, pp. 301-305.
- [41] Emery, X. (2005) Simple and Ordinary Kriging Multigaussian Kriging for Estimating recoverable Reserves. *Math Geol*, v. 37, pp. 295-319.
- [42] Hormozi, H., Hormozi, E., Rahimi Nohooji N. (2012) The Classification of the Applicable Machine Learning Methods in Robot Manipulators. *Int J of Mach Learning and Computing*, v. 2, pp. 560-563.
- [43] Lefohn, A.S., Knudsen H.P. (2011) Using Ordinary Kriging to Estimate the April - September 24-Hour W126 and N100 Ozone Exposure Metrics for 2010 for the United States.
- [44] Shademan Khakestar, M., Madani, H., Hassani, H., Moarefvand, P. (2013) Determining the best search neighbourhood in reserve estimation, using geostatistical method: A case study anomaly No 12A iron deposit in central Iran. *J Geol. Soci., India*, v. 81, no. 4, pp. 581-585.
- [45] Chilès, J.P., Delfiner, P. (1999) *Geostatistics: Modeling Spatial Uncertainty*. Wiley, New York. pp. 695p.
- [46] Soltani Mohammadi, S., Hezarkhani, A., Tercan, A.E. (2012) Optimally locating additional drill holes in three dimensions using grade and simulated annealing. *J Geol. Soci. India*, v. 80, no. 5, pp. 700-706.
- [47] Goovaerts, P. (1997) *Geostatistics for Natural Resources Evaluation*. Oxford University Press, New York. 496 p.
- [48] VerHoef, J.M., Cressie, N. (1993) Multivariable spatial prediction. *Math Geol*, v. 25, pp. 219-239.
- [49] Calder, C.A., Cressie, N. (2009) *Kriging and Variogram Models*. Elsevier Ltd. All rights reserved, pp. 49-55.
- [50] Babak, O., Insalaco, E., and Henriquel, P. (2011) On Relationship between Spatial Continuity and the Average Grade in Ore post Ore-Waste Discrimination. Recovery, CSPG CSEG CWLS Convention.
- [51] Sakata, S., and Ashida, F. (2004) An efficient algorithm for Kriging approximation and optimization with large-scale sampling data. *Comput. Methods Appl. Mech. Engrg.* v. 193, pp. 385-404.
- [52] Brus, D., Heuvelink, G.B.M. (2007) Optimization of sample patterns for universal kriging of environmental variables. *Geoderma*, v. 138, pp. 86-95.
- [53] David, M. (1970b) Geostatistical ore reserve calculation, a step by step case study, 1 Xth International Symposium for Decision-Making in the Mineral Industry. C.I.M.M. Special Vol, no. 12, Montreal.
- [54] Journel, A. (1993) Geostatistics: roadblocks and challenges, in A. Soares, ed., *Geostatistics-Troia*, v. 1, Kluwer, pp. 213-224.
- [55] Verly G (1984) Estimation of Spatial Point and Block Distributions: The MultiGaussian Model, PhD thesis, Stanford University, Stanford, CA.
- [56] David, M. (1970c) *Geostatistical Ore Reserve Estimation*, Amsterdam, Elsevier, 283 p.
- [57] Boniol, D., Toth D. (1999) *Geostatistical Analysis: Water Quality Monitoring Network for the Upper Floridan Aquifer in East-Central Florida*. Technical Publication SJ99-1, St. Johns River Water Management District Palatka, Florida.
- [58] Wober, H. H., Morgan, P. J. (1993) Classification of ore reserves based on geostatistical and economic parameters, *CIM Bulletin*, v. 86, pp. 73-76.
- [59] Noppé, M.A. (1994) *Practical Geostatistics for on-Site Analysis - A Coal Example*. Mining Geostatistics Conference, Geostatistical Association of South Africa, Kruger National Park, South Africa.
- [60] Yamamoto, J., DA Rocha, M. 1996. REVISÃO E RECOMENDAÇÕES PARA O CÁLCULO E CLASSIFICAÇÃO DE RESERVAS MINERAIS. *Revista Brasileira de Geociências*, 26(4): 243-254
- [61] Ortiz, J. M., Emery, X. (2004) Categorización de recursos y reservas mineras, in Magri, E., Ortiz, J.M., Knights, P., Henríquez, F., Vera, M., and Barahona, C., eds., 1st International Conference on Mining Innovation MININ, 2004: Gecamin Ltda, Santiago, p. 198-208
- [62] JORC (2012) Australasian Code for Reporting of Identified Mineral Resources and Ore Reserves (The JORC Code), The Joint Ore Reserves Committee of the Australasian Institute of Mining and Metallurgy, Australian Institute of Geoscientists, and Minerals Council of Australia.
- [63] Li, S., Dimitrakopoulos, R., Scott, J., Dunn, D. (2008) Quantification of geological uncertainty and risk using stochastic simulation and applications in the coal mining industry. *Ore Body Model Strategic Mine Plann Spectrum Ser*, v. 14, pp. 253-260.
- [64] Asghari, O., Madani Eshfahani N. (2013) A new approach for the geological risk evaluation of coal resources through a geostatistical simulation Case study: Parvadeh III coal deposit. *Arab J Geosci*, v. 6, pp. 957-970.